

Multispectral-Polarimetric Sensing for Detection of Difficult Targets.

W A Hubbard, F T Gowen, G J Bishop
BAE SYSTEMS Advanced Technology Centre
Filton, Bristol, BS34 7QW

G Innes, D J Jordan, D Hayter, J Ellis
QinetiQ
Malvern, Worcestershire WR14 3LG

Abstract

The benefits for the detection of difficult targets have been demonstrated for multispectral and polarimetric imagery in differing conditions. The spectral differences between target and background have been seen to provide an enhancement to target discrimination. However, false alarms can occur mainly due to spectral variations in background materials. Complimentarily, polarimetric imagery has been used to detect man made targets by exploiting the reflective characteristics of man-made objects and the suppression of background clutter; but polarimetric imagery for a detection process can be limited by the geometry and nature of targets. The intention of this work has been to investigate whether adding the polarimetric to the multispectral information decreases background induced false alarms whilst maintaining good detection statistics for low contrast targets in the SWIR and LWIR wavebands.

Keywords: Multispectral, Polarimetric, Detection of Difficult Targets, SWIR

Introduction

Studies have shown that in differing conditions multispectral [1] and polarimetric [2] sensors can enhance target detectability. It has been demonstrated that multispectral imagery can be used to detect low contrast targets using intrinsic spectral differences between target and background. However, multispectral imagery can produce false alarms mainly caused by spectral variations in background materials. Polarimetric imagery has been used to detect man made targets by exploiting the surface finish of these objects compared to the background. However, the performance of polarimetric imagery in isolation can be limited by the geometry and nature of targets. By adding the polarimetric information to the multispectral it may be possible to decrease background induced false alarms whilst providing good detection statistics for low contrast targets.

This study considers if false alarm rates and target detection can be improved if the polarimetric content of the scene is employed in addition to spectral content in the detection process in the LWIR and SWIR wavebands.

The LWIR waveband is of significant military importance because of its 24 hour operating capability. However, sensors operating in this waveband are relatively complex and expensive, and a multispectral-polarimetric sensor would be considerably more complex still. Consequently, before embarking on the building (or even the design) of such a sensor, it is important to be able to model its likely performance and hence determine its potential advantages. A model in the LWIR has been developed for this work, and results from performance testing with simple synthetic imagery have been gathered.

Camera technology is simpler, cheaper and better developed in the SWIR waveband, and several operational hyperspectral sensors are commercially available. Moreover, it has been observed that a SWIR hyperspectral sensor is particularly effective at defeating targets employing Camouflage Concealment and Deception (CC&D) techniques, as these are conventionally aimed at visual wavelengths. These sensors have also been shown to detect land mines. A simple SWIR polarimetric sensor has been constructed, based around an Indium Gallium Arsenide camera operating in the 1 – 1.7 micron waveband. Polarisation signatures have been measured from a small number of static targets at short range in the SWIR waveband. Key findings of this work are that the measured polarisation signatures of a painted panel at various orientations are in broad agreement with those predicted by polarimetric theory. In addition SWIR model development has been carried out for two weather conditions where some simplifications can be made, namely completely overcast and full sun, blue sky, conditions. Due to the complexity of modelling SWIR polarimetric signatures, validation measurements are critical, and these have commenced; first results are reproduced herein.

The radiance values for all modelling, at each waveband and for each polarisation, were collected by running suitable scenarios through the BAE SYSTEMS SIRUS infrared predictive tool. It incorporates surface optical properties including spectrally-dependent or complex BDRF 'paints', and atmospheric / environmental contributions by including an embedded version of the standard MODTRAN code. Surface temperature is imported as part of the surface model geometry. SIRUS has been used extensively by BAE SYSTEMS Air Systems, Warton for L.O. Studies, and validated against M.o.D supported engine, plume and surface

optics trials and studies (RAPS, Mohican and SOAR).

LWIR Modelling

The modelling has been undertaken for the waveband 8 μm to 10.4 μm , with six 0.4 μm sub-bands for the multispectral analysis [3].

Two approaches were investigated for material descriptions to be input to the model. One was a Fresnel model of the materials, containing two parts, a diffuse parameter and refractive index terms (n and k) which generate specular behaviour and are applied according to the Fresnel equations applicable at material boundaries. Background materials were modelled by setting the diffuse parameters to available bandwidth averaged measured Hemispherical Directional Reflectance (HDR) data; thereafter setting the refractive index n component for a small apparent temperature difference between the orthogonal polarisations when viewed at 45° incidence, to provide some small amount of specularity. The k component of the refractive index was set to zero. The target paint material was subsequently modelled by selecting a slightly larger value for the refractive index n component, and selecting a value for the diffuse parameter to give the same emissivity in the unpolarised broadband, at normal incidence as the background. The second approach was to extract parameters from measured HDR polarimetric data to fit to a cosine polynomial model of the reflectances, and hence determine apparent radiance values. The data was fitted to a model of purely specular reflection.

With each of these approaches the contrast between target objects and background were reduced to provide difficult cases for the detection processing. All modelling performance assessments were completed with a 1976 US Standard atmosphere, as defined in Modtran.

Image multispectral cubes were constructed of background with variability applied and

flat green-painted targets embedded for each of the s-polarisation and p-polarisation data, and thereafter for each of the Stokes parameters S_0 and S_1 . S_0 is the total intensity, given by the sum of the intensities measured using two orthogonal linear polariser orientations. S_1 is the difference in intensities, and is zero for unpolarised radiation. Variability in the background was applied by assuming a random surface orientation between values of 0° to 90° incidence. Single pixel targets were embedded in each of the background types at a range of surface orientations, and at each of the sub-bands. The Rx algorithm was applied with a target window of size five pixels. The image multispectral cubes were converted to apply to a standard multispectral imager, and subsequently had a generic sensor noise term added [3]. The final image multispectral cubes were passed through the Multispectral Rx detection algorithm [4], and detection statistics in the form of Receiver Operator Characteristics (ROC) curves collected.

For Fresnel material modelling, results are presented for image multispectral cubes calculated for a target range of 3 km, and target incidence angles of 45° (Figure 1) and 70° (Figure 2). Five hundred image cubes were created and processed for each case. The figures show that an increased angle of incidence to the target increased the performance for the s-polarisation (s), and hence the S_1 (polarised) multispectral image cubes. This is expected behaviour as the angle approaches the Brewster angle. The S_1 (diffpol) imagery provided significantly better performance in both cases, being perhaps slightly increased at 70° incidence.

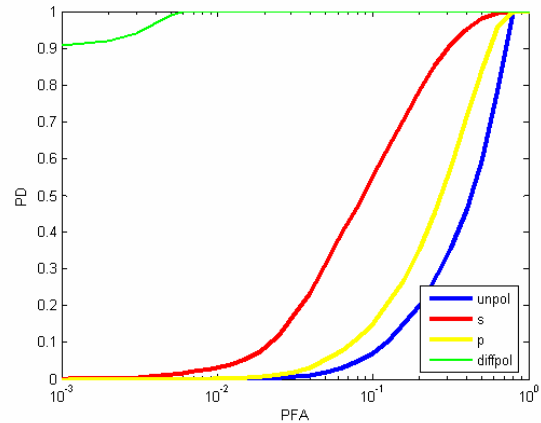


Figure 1 – Plate Target (45 Degrees)

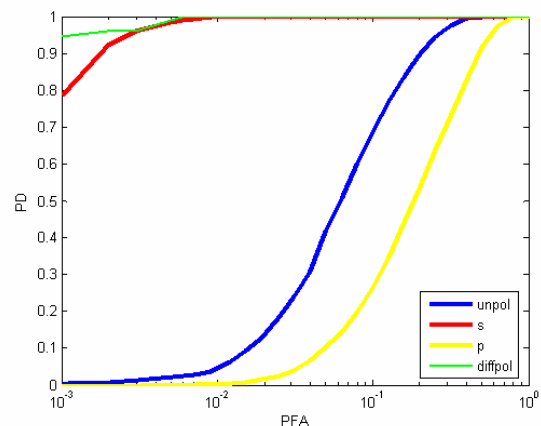


Figure 2 – Plate Target (70 Degrees)

For cosine polynomial material modelling, results are presented for image multispectral cubes calculated for a target range of 5 km. The target was an extended multi-faceted object (the geometry of a generic tank has been used), and output images were collected at a high resolution and de-resolved for the scenarios to be modelled to generate random object placement with respect to pixels, and a mean value taken to give the object effectively lying in a single pixel. One hundred image cubes were created and processed for each case. Gains due to the addition of polarisation information are seen when the target viewing angle is 45° (Figure 3) and most significantly at 30° (Figure 4), for s-polarisations and the S_1 Stokes parameter.

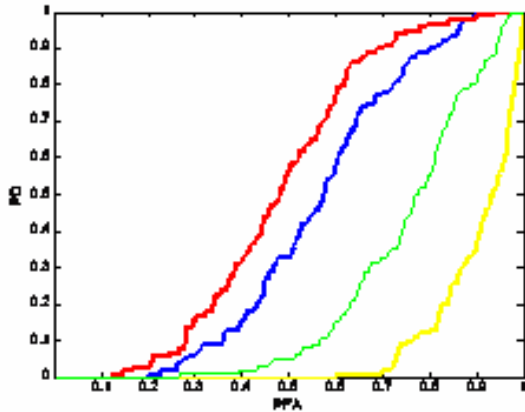


Figure 3 – Tank Target (30 Degrees)

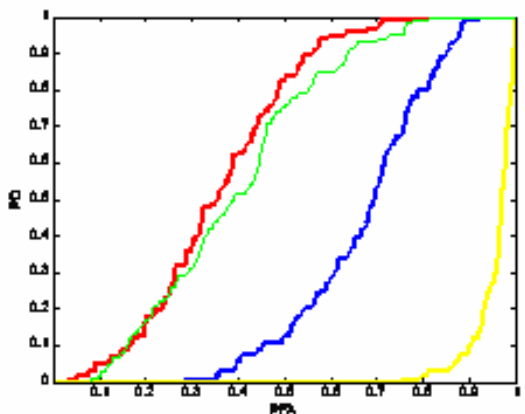


Figure 4 – Tank Target (45 Degrees)

SWIR Sensor Build

The sensor used is based on a 320x240 pixel Sensors Unlimited 12 bit digital InGaAs camera operating between 1 μ m and 1.7 μ m. A polariser fitted into a hand-operated rotation stage is used as the analyser. The scale of this project has not permitted the construction of a sensor that could acquire the polarisation sub-images simultaneously. All components in the sensor are attached to a metal base plate, enclosed in a light-tight box, which in turn is mounted on a tripod. The integration time of the camera is controlled through a hyperterminal. Any additional compensation for light levels is addressed through the use of neutral density filters. In operation the polariser was rotated through 0°, 45° and 90°. At each step one image was acquired. Manipulations of the resulting images permitted the relevant

Stokes parameters to be determined for each pixel. It took approximately 20 seconds to acquire each image. Unfortunately, the relatively small number of pixels in the InGaAs camera used in the sensor, coupled with the large field of view lens (40°) with which it was equipped, resulted in a low spatial resolution sensor. This in turn limited the range and/or the size of targets that could be used in data gathering exercises. In order to permit longer ranges, or smaller targets to be used, the camera lens has since been replaced by a smaller field of view (7.6°) conventional glass camera lens. Figures 6 and 7 show corresponding intensity and polarimetric images of vehicles, in the shadow of a building, at a range of 100 m. The vehicles, shown circled, are more readily apparent in the polarimetric image



Figure 5. Intensity image of vehicles in shadow



Figure 6. Polarimetric image of vehicles in shadow

Joint SWIR Sensor – Hyperspectral Sensor Trials

Data was gathered by QinetiQ at regular intervals over a two day period in tandem with a hyperspectral imager provided and operated by BAE SYSTEMS ATC. A typical target scene is shown in RGB (Figure 7), and with the SWIR sensor (Figure 8) with all targets labelled (shading around the image is vignetting caused by the polariser in front of the imaging lens, as the clear aperture of the polariser is smaller than that of the imaging lens being used). A number of small targets were placed on grass and viewed from a distance of 19.8m at an elevation of 5.34m from a north-facing laboratory window. The panel was mounted at 30° elevation and 0° azimuth for the duration of the trial. This arrangement was chosen because the time taken to acquire each image (approximately one minute for the hyperspectral data) limited the number of different data sets which could be addressed.



Figure 7 – RGB Image of Scene

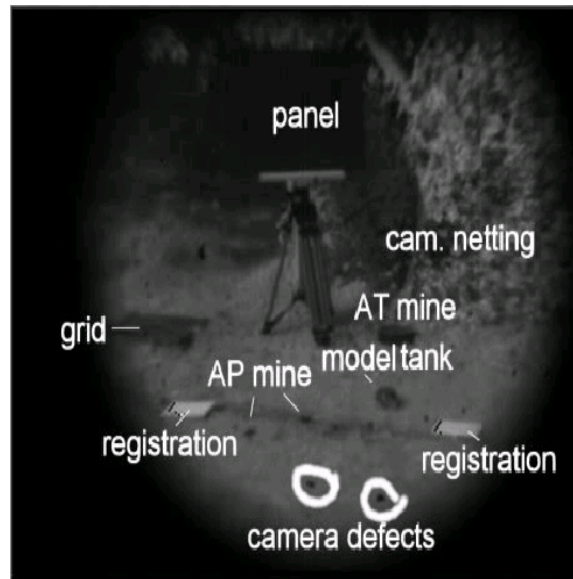


Figure 8 – SWIR Sensor Image

On both days of the trial the illumination conditions were constant, day one being overcast and day two being bright, clear sky. Twenty images were taken over two days, each of which was processed individually. The only moving parts of the scene were foliage in the background, which therefore show false polarimetric data in the processed images. The camera was mounted on a tripod and images taken with the polariser oriented at 0°, 45° and 90°. These images were stored digitally on a PC which was later used to process them in order to obtain polarimetric images. Additional processing was carried out in order to highlight targets in the scene.

Figure 9 is an S_0 (intensity) image and a scaled S_0 image. Scaling has been applied to mark the scene content according to grey scale levels. It can be seen that while scaling an S_0 image highlights the small targets, non-target objects (leaves, camera defects etc) are equally highlighted.

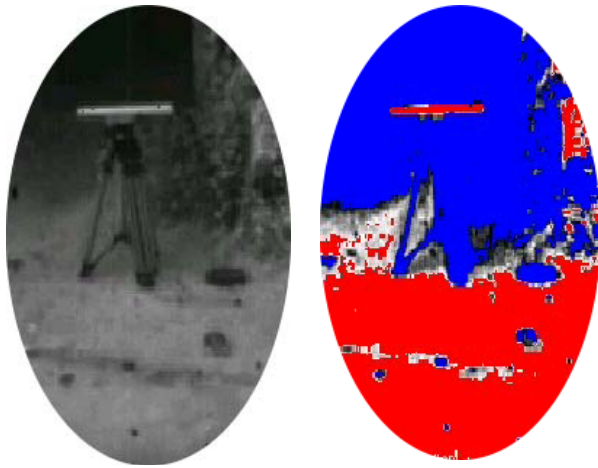


Figure 9 – SWIR Intensity Image

Figure 10 is an S_1/S_0 image and a scaled S_1/S_0 image. It can be seen that scaling this image highlights man-made objects exclusively. The panel, mines and tripod legs are clearly visible, while natural objects and camera defects are ignored. (Note: some vegetation is highlighted as it has moved between the sequential image gathering).

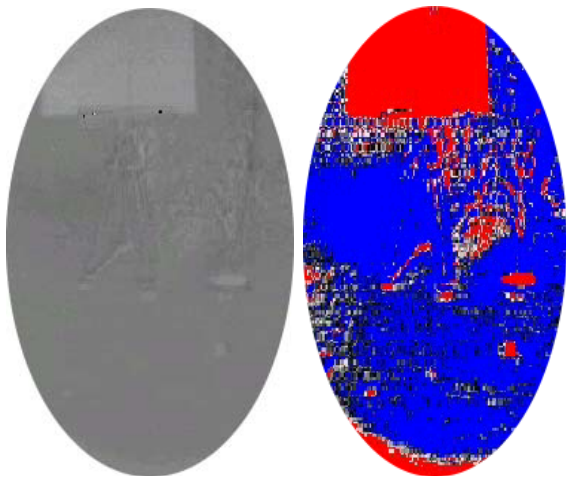


Figure 10 – Scaled S_1/S_0 image

SWIR images at 1.06 μm (Figure 11) and at 1.50 μm (Figure 12) were taken with the hyperspectral camera and demonstrate that judicious selection of the spectral content assists object identification. For example, at 1.06 μm wavelength the AP and AT mines can be easily seen, and at 1.5 μm the camouflage net is distinct from the natural

vegetation.



Figure 11 – 1.06 μm Image



Figure 12 - 1.5 μm Image

SWIR Modelling and Validation

In the 1 – 1.7 μm waveband modelling was completed as for the LWIR, although material modelling was conducted for the cosine polynomial model only. Polarised HDR data was available at limited angles of incidence (40° and 60°), and unpolarised data was available at 8° incidence. Fitting was completed for six sub-bands, and in order to conduct the fitting it was assumed that at 8° incidence the p and s-polarisations contributions were equal, and additional points were inferred by setting 0° at the same values for 8° , and assuming 100% reflectivity at 90° . A diffuse term was also included in the material description for processing in SIRUS. Calibration data for the sensor is not currently available; hence it is not possible to validate absolute radiance values at this time. General behaviour and trends are considered here. Calibration is planned once final filter selection has been completed.

Data on the polarimetric signature of a painted panel was gathered as a function of zenith and azimuth angle, to be compared with the SIRUS IR signature prediction.

The panel was viewed at a distance of approximately 12m from the north-facing door of a laboratory. Data was gathered for zenith angles of 15°, 30°, 45°, 60° and 75° at azimuth angles of 0° and 30°. Early data analysis indicated that there was non-uniformity across the part of the panel being analysed. Further investigations concluded that this was due to a slight difference in the optical properties of the paint across the surface. This was deemed not to be significant as data for each measurement was averaged over a number of pixels, varying between 36 and 100 depending on the visible area of the panel. 27 sets of data were collected. These were sorted according to whether or not there was direct sun on the panel. Standard Error bars were included in the results.

For the cases of no direct sun, the SIRUS Model was executed without direct sun, however solar multi-scattering effects have been included for a total cloud cover of Stratus/Strato-Cumulus (base at 0.66 km and top at 2 km). The corresponding trial results are for periods over two days and therefore the actual sun position would have varied. Figure 13 gives the results from modelling with overcast sky conditions, with the corresponding trials results in Figure 14. The results are broadly in agreement with polarimetric theory; under uniform conditions one would expect to see the polarimetric signature dropping to zero at normal incidence, rising as the panel moves out of plane in any direction and peaking at the Brewster angle for the particular material being viewed. The signature would then begin to drop again as the viewing angle approaches grazing. It can be seen that gross behaviour of the Degree of Linear Polarisation (DOLP) i.e. S_1/S_0 , is comparable, in that the response rises and peaks at 30° zenith angle, then falls. The results between the model and trial vary in the main as the model predicts that the 30° azimuth DOLP should remain above that at 0° azimuth at zenith angles greater than 30°, whereas the trials results

show the corresponding values dipping below those at 30° azimuth.

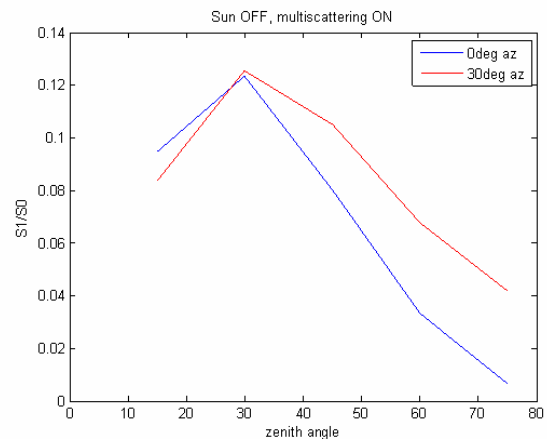


Figure 13 – SWIR Modelling Results (Occluded Conditions)

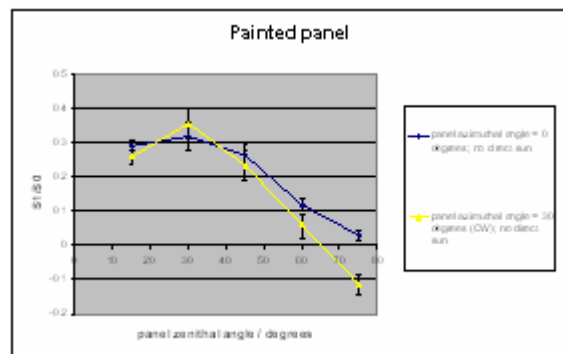


Figure 14 – SWIR Experimental Results (Occluded Conditions)

Illumination was defined as direct sunlight if no cloud obscured the sun during measurement. However, on no occasion were there completely cloudless conditions. Consequently, movement of cloud during measurement could introduce false readings by changing the illumination conditions. These false readings were identified by a combination of analysing the data and observing cloud movement throughout the measurements. They were identified by comparing the set of images taken from any particular run and locating any non characteristic discontinuities in intensity. An estimate of the cloud coverage was recorded along with the data, and it was seen that a consistent trend appeared in the data when cloud cover was less than 20%. Figure 15 gives the results from modelling with clear sky conditions with a 50%

diffuse component in the material modelling, with the corresponding trials results in Figure 16. A significant diffuse component to the material modelling improves the match of the gross behaviour of the DOLP with the measured trials values. Notable exceptions are that the results of modelling DOLP for times of day 11.30 and 14.20 are approximately the same, which would be expected as a due north line of sight gives sun positions approximately symmetrical about that direction and sun positions at the same elevations. In addition, the modelled values at 15.50 do not lie completely below the other modelled results, as is seen in the trials results; however it can be seen that the results for 15:50 are slightly ‘flatter’, which is seen in the trials results.

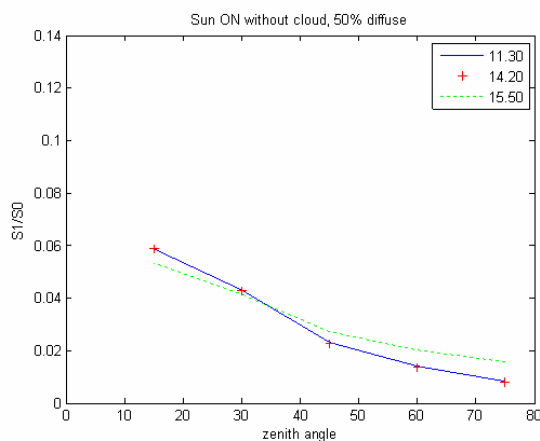


Figure 15 – SWIR Modelling Results (Clear Sky)

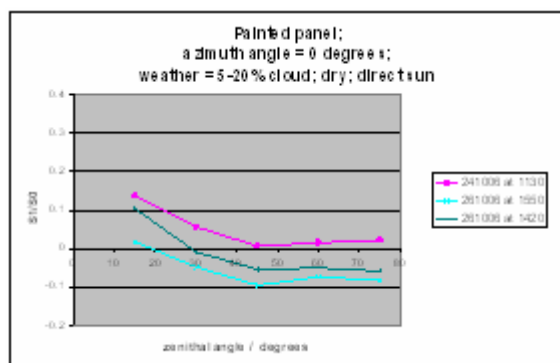


Figure 16 – SWIR Experimental Results (Clear Sky)

Conclusions

Results from the LWIR modelling of difficult targets indicate that the addition of polarimetric information to multispectral image data provides an enhancement to detection performance, particularly when the target of interest is of a simple construction and appears at advantageous parts of the scene, i.e. away from normal angles.

An experimental SWIR polarimetric sensor has been built and trial imagery taken. A joint trial with a Hyperspectral sensor has demonstrated the gains to be achieved from both polarimetric and spectral information. S_1 images taken so far in SWIR suggest that polarisation offers advantages in the SWIR in picking out targets from cluttered backgrounds. Targets imaged are more easily distinguished from stationary background, even by applying a simple scaling process. The same process when applied to a non-polarimetric image fails to highlight targets satisfactorily whilst remaining robust against false alarms. A SWIR Model has been developed, and validation against trials imagery is underway and providing initial gross agreements.

References

- 1 G.Bishop and A.Killey “Final Report on RCSC18 Sensor Technologies for Future Tactical UAVs Research Study”. TES100935 Sept. 2006
- 2 D Jordan, G Innes and D Hayter “Polarimetric Imaging”. Journal of Defence Science, Vol. 10, No. 3, R166-172 (2005)
- 3 Eismann et al. “Comparison of Infrared Imaging Multispectral Sensors for Military Target Detection Applications”. SPIE Vol. 2819 / 95.
- 4 I.S.Reed and X.Yu “Adaptive Multi-band CFAR Detection of an Optical Pattern Unknown Spectral Distribution”. IEEE Trans. Acoustics, Speech, Signal

Processing, Vol. 38, pp.1760-1770, Oct.
1990

Acknowledgements

The work reported in this paper was funded by the Electro-Magnetic Remote Sensing (EMRS) Defence Technology Centre, established by the UK Ministry of Defence and run by a consortium of SELEX Sensors and Airborne Systems, Thales Defence, Roke Manor Research and Filtronic